

**TOME 24**

RVCMA824



**1987**

**Revue  
de  
Chimie minérale**

**gauthier-villars**

## Table des matières

---

<b>Les transitions de phases des oxyfluorures <math>A_3TiOF_5</math> et <math>A_3MO_2F_4</math> (<math>A=K, Rb, Cs; M=Nb, Ta</math>).</b>	
M. FOUAD, J. P. CHAMINADE, J. RAVEZ & P. HAGENMULLER . . . . .	1
<b>Étude structurale par spectroscopie Mössbauer et rayons X de spinelles lacunaires de type <math>In_2S_3</math>.</b>	
C. ADENIS, J. OLIVIER-FOURCADE, J.-C. JUMAS & E. PHILIPPOT . . . . .	10
<b>Nouveaux résultats sur les apatites azotées. I. — Le type <math>Ln_{10}Si_6N_2O_{24}</math> relatif au cérium.</b>	
J. GAUDÉ . . . . .	22
<b>The structure of some ternary phases of calcium.</b>	
A. IANDELLI . . . . .	28
<b>Nouveaux oxydes à structure en couches dérivant de celle de la pérovskite : le titanate double, <math>Na_2Gd_2Ti_3O_{10}</math> : cristallochimie et réactions d'échange.</b>	
M. GONDRAND & J.-C. JOUBERT . . . . .	33
<b>Étude magnétique de <math>Fe_3(PO_4)O_3</math> avec notamment des effets de covalence et de frustration.</b>	
G. GAVOILLE, C. GLEITZER & G. J. LONG . . . . .	42
<b>Étude cristallochimique de trisoxalato-metallates (III) de cations monovalents. II. Cas de <math>(NH_4)_3[Fe(C_2O_4)_3] \cdot 3H_2O</math>.</b>	
E. H. MERRACHI, B. F. MENTZEN, F. CHASSAGNEUX & J. BOUIX . . . . .	56
<b>Caractérisation des degrés d'oxydation de fer par méthodes spectrométriques. A. Oxydes spinelles à un sous-réseau de valence mixte.</b>	
B. HANNOYER, M. LENGLLET & J. C. TELLIER . . . . .	68
<b>Caractérisation des degrés d'oxydation du fer par méthodes spectrométriques. B. Oxydes spinelles à deux sous-réseaux de valence mixte.</b>	
M. LENGLLET, J. ARSENE & F. JEANNOT . . . . .	81
<b>Ein neues Oxoplumbat (IV): <math>CsNa_3[PbO_4]</math>.</b>	
H. STOLL & R. HOPPE . . . . .	96

## Table des matières

---

<b>Préparation et propriétés optiques de nouveaux matériaux amorphes obtenus par hypertrempe dans les systèmes binaires de difluorures.</b>	
G. DEMORTAIN, A. TRESSAUT, B. TANGUY, J. PORTIER & P. HAGENMULLER . . . . .	117
<b>Nouveaux verres fluorés à base d'indium.</b>	
A. BOUAGGAD, G. FONTENEAU & J. LUCAS . . . . .	129
<b>Influence des paramètres expérimentaux sur la dévitrification du verre <math>\text{Li}_2\text{B}_2\text{O}_4</math> 0,9 – <math>\text{LiFe}_5\text{O}_8</math> 0,1 (% mol).</b>	
C. MARTIN, C. CHAUMONT & J. C. BERNIER . . . . .	139
<b><math>\text{Rb}_{x}\text{P}_8\text{W}_8\text{O}_{40}</math> : Un bronze-diphosphate de tungstène à tunnels octogonaux. Étude structurale comparée avec <math>\text{CsP}_8\text{W}_8\text{O}_{40}</math>.</b>	
M. LAMIRE, Ph. LABBE, M. GOREAUD & B. RAVEAU . . . . .	153
<b>Ordre à courte distance dans les solutions solides de type fluorine excédentaire en anions <math>\text{Ca}_{1-x}\text{M}_x^{\text{IV}}\text{F}_{2+2x}</math> (<math>\text{M}^{\text{IV}} = \text{U}, \text{Zr}</math>).</b>	
J.-P. LAVAL, A. MIKOU & B. FRIT . . . . .	165
<b>Le manganèse IV à l'état isolé au sein d'un oxyde de structure <math>\text{K}_2\text{NiF}_4</math>: <math>\text{Sr}_{0,50}\text{La}_{1,50}\text{Li}_{0,50}\text{Mn}_{0,50}\text{O}_4</math>.</b>	
G. DEMAZEAU, Eun-ok OH-KIM, Kai-tai WANG, L. FOURNES, J.-M. DANCE, M. POUCHARD & HAGENMULLER . . . . .	183
<b>Nouveaux hydruroaluminates de potassium à structure elpasolite obtenus sous haute pression.</b>	
J. BASTIDE, P. CLAUDY, J.-M. LETOFFE, & J. EL HAJRI . . . . .	190
<b>Structural chemistry of phyllo manganates: Experimental evidence and structural models.</b>	
P. STROBEL & J.-C. CHARENTON . . . . .	199
<b>NMR-Untersuchungen an Aluminoborat-Gläsern.</b>	
M. HÄHNERT & E. HALLAS. . . . .	221
<b>Synthèse et Étude d'hydrogénophosphates de formule <math>\text{MHPO}_4</math>, <math>3\text{H}_2\text{O}</math> et <math>(\text{MHPO}_4)_2</math>, <math>3\text{H}_2\text{O}</math> (<math>\text{M} = \text{Co}, \text{Ni}, \text{Zn}</math>).</b>	
Y. CUDENNEC, A. LECERF, A. RIOU & Y. GERAULT . . . . .	234
<b>Préparation et caractérisation du tétrahydruroaluminate de potassium <math>\text{KAlH}_4</math>.</b>	
J.-P. BASTIDE, P. CLAUDY, J.-M. LETOFFE & J. EL HAJRI . . . . .	248



## Table des matières

---

<b>Étude du système CsF-LuF<sub>3</sub>.</b>	
J. METIN, D. AVIGNANT & J. C. COUSSEINS . . . . .	267
<b>Structure cristalline de K<sub>5</sub>Nb<sub>6</sub>Zr<sub>2</sub>P<sub>5</sub>O<sub>34</sub>.</b>	
S. DENIARD-COURANT, Y. PIFFARD & M. TOURNOUX . . . . .	276
<b>Influence du degré d'ordre cationique sur les propriétés diélectriques de quelques phases de type «bronzes quadratiques de tungstène».</b>	
J. THORET & J. RAVEZ. . . . .	288
<b>Fluorures complexes de cuivre (II) VI<sup>(1)</sup> Structure cristalline de Ba<sub>7</sub>CuFe<sub>6</sub>F<sub>34</sub>.</b>	
J. RENAUDIN, G. FEREY, A. D. KOZAK ET & M. SAMOUËL . . . . .	295
<b>Synthesis and characterization of new mixed oxohalides of antimony and tellurium.</b>	
A. JEREZ, C. PICO, M. VEIGA & J. ALONZO . . . . .	305
<b>Quelques nouveaux exemples de phases à couches d'antiprismes quadratiques MX<sub>8</sub> ou de polyèdres MX<sub>9</sub>.</b>	
A. MIKOU, J.-P. LAVAL & B. FRIT. . . . .	315
<b>Propriétés de conduction ionique des solutions solides Cd<sub>1-x</sub>In<sub>x</sub>F<sub>2+x</sub> et Cd<sub>1-x</sub>Bi<sub>x</sub>F<sub>2+x</sub>.</b>	
P. LAGASSIE, J. GRANNEC, M. EL OMARI & J.-M. REAU . . . . .	328
<b>Étude cristallochimique et optique des systèmes Na<sub>3</sub>Ln(PO<sub>4</sub>)<sub>2</sub>-K<sub>3</sub>Ln(PO<sub>4</sub>)<sub>2</sub> (Ln=Eu, Gd).</b>	
M. MESNAOUI, M. MAAZAZ, Z. JIN CHAO, C. PARENT, R. OLAZCUAGA, G. LE FLEM & P. HAGENMULLER. . . . .	338
<b>Intercalation d'amines secondaires et tertiaires dans l'oxyde lamellaire HTiNbO<sub>5</sub>.</b>	
A. GRANDIN, M. M. BOREL & B. RAVEAU. . . . .	351
<b>Étude structurale de N<sub>2</sub>H<sub>5</sub>Sn<sub>2</sub>F<sub>5</sub>.</b>	
S. VILMINOT, W. GRANIER, H. WAHBI & L. COT . . . . .	362





## Table des matières

<b>Réaffinement et nouvelle analyse de la structure de W<sub>18</sub>O<sub>49</sub>.</b>	
M. LAMIRE, P. LABBE, M. GOREAUD & B. RAVEAU . . . . .	369
<b>The crystal structure of 18-crown-6 complexes of hydrated lithium chloride and bromide.</b>	
T.-L. CHANG, M. ZHAO, N.-H. HU & Z.-S. JIN . . . . .	382
<b>Structure cristalline du fluorure LiTiZr<sub>5</sub>F<sub>22</sub>.</b>	
D. AVIGNANT, E. CAIGNOL, R. CHEVALIER & J. C. COUSSEINS . . . . .	391
<b>Cristallochimie du couple Cu(II)-Ti(IV) dans les oxydes ABO<sub>3</sub> des familles corindon, bixbyite et pérovskite.</b>	
P. MOURON, N. NGUYEN & J. CHOISNET . . . . .	401
<b>Polymorphisme de l'iodure de césum et de cadmium.</b>	
V. TOUCHARD, M. LOUËR, J. AUFRÉDIE & D. LOUËR . . . . .	414
<b>Étude cristallochimique comparative de trisoxalato-metallates (III) de cations monovalents.</b>	
<b>III. Cas de Rb<sub>3</sub>[Cr(C<sub>2</sub>O<sub>4</sub>)<sub>3</sub>], 3H<sub>2</sub>O.</b>	
El. H. MERRACHI, B. F. MENTZEN & F. CHASSAGNEUX . . . . .	427
<b>Preparation, crystal structure, and thermal behaviour of potassium ozonide.</b>	
W. SCHNICK & M. JANSEN . . . . .	446
<b>Synthesis, characterization and crystal structure of <i>mer</i>(dien)-<i>syn</i>(H, NO<sub>2</sub>)-(diethylenetriamine)-(ethylenediamine) nitrocobalt (III) tetrachlorozincate (II).</b>	
K. ANDJELKOVIĆ, R. HERAK, N. JURANIĆ, L. MANOJLOVIĆ-MUIR & M. CELAP . .	457
<b>NaTi<sub>5</sub>NbO<sub>13</sub>, phase de type A<sub>2</sub>Ti<sub>6</sub>O<sub>13</sub> déficiente en cations alcalins synthétisée par chimie douce.</b>	
A. GRANDIN, M. M. BOREL & B. RAVEAU . . . . .	470
<b>Comportement sous haute pression d'orthophosphates mixtes de calcium et de cobalt Ca<sub>3-x</sub>Co<sub>x</sub>(PO<sub>4</sub>)<sub>2</sub>, 0,40 &lt; x ≤ 3.</b>	
THÉODORET, J. LENZI, P. ROUX, G. BONEL & M. LENZI . . . . .	478

## Table des matières

---

<b>Étude du diagramme ternaire H<sub>2</sub>O – (NH<sub>4</sub>)<sub>3</sub>[Cr(C<sub>2</sub>O<sub>4</sub>)<sub>3</sub>] – (NH<sub>4</sub>)<sub>3</sub>[Fe(C<sub>2</sub>O<sub>4</sub>)<sub>3</sub>] isothermes 25 et 70°C.</b>	
E. A. MERRACHI, F. CHASSAGNEUX, R. COHEN-ADAD & B. F. MENTZEN . . . . .	489
<b>Single crystal structure of NH<sub>4</sub>CuMoS<sub>4</sub>.</b>	
W. BENSCH, G. STAUBER-REICHMUTH, A. RELLER & H. R. OSWALD . . . . .	503
<b>Influence de la dimensionnalité caractérisant l'assemblage des polyèdres de coordination de l'europium ou du terbium sur les migrations d'énergie dans les borates Li<sub>6</sub>Gd<sub>1-x</sub>Eu<sub>x</sub>(BO<sub>3</sub>)<sub>3</sub>, Na<sub>3</sub>Gd<sub>1-x</sub>Ln<sub>x</sub>(BO<sub>3</sub>)<sub>2</sub> (Ln = Eu, Tb) et Gd<sub>1-x</sub>Eu<sub>x</sub>B<sub>3</sub>O<sub>6</sub>.</b>	
F. W. TIAN, A. GARCIA & C. FOUASSIER. . . . .	509
<b>The KH-MgH<sub>2</sub> system.</b>	
H.-H. PARK, M. PEZAT, J. DARRIET & P. HAGENMULLER . . . . .	525
<b>Élaboration de céramiques de titanate de magnésium MgTiO<sub>3</sub>, à partir d'un précurseur organométallique.</b>	
S. EL HADIGUI, S. VILMINOT & P. POIX. . . . .	531
<b>Les variétés « bronze de tungstène hexagonal » des trifluorures CrF<sub>3</sub> et VF<sub>3</sub>.</b>	
R. DE PAPE, A. LE BAIL, F. LUBIN & G. FEREY. . . . .	545
<b>Étude cristallochimique des chromates doubles de zinc et d'alcalins.</b>	
H. SUQUET & S. LAUNAY. . . . .	552
<b>A new model structure of sheet sodium (Na) Silicate Hydrates (Na-SH); theoretical view based on known X-ray and NMR-measurements.</b>	
A. BRANDT, W. SCHWIEGER & K.-H. BERGK . . . . .	564
<b>Synthesis of first stage graphite intercalation compounds with fluorides.</b>	
S. MOURAS, A. HAMWI, D. DJURADO & J.-C. COUSSEINS . . . . .	572
<b>Étude de la transition de phases de nouveaux oxyfluorures ferroélastiques K<sub>3</sub>NbOF<sub>6</sub> et K<sub>3</sub>TaOF<sub>6</sub>.</b>	
M. FOUD, J. RAVEZ, J. P. CHAMINADE & P. HAGENMULLER . . . . .	583



## Table des matières

**Amélioration de la qualité cristalline de la berline : solubilité et croissance en milieu sulfurique.**

A. GOIFFON, J.-C. JUMAS, C. AVINENS & E. PHILIPPOT . . . . . 593

**Ein neues Erdalkalimetall-Oxoindat der Formel BaSr<sub>2</sub>In<sub>2</sub>O<sub>6</sub>.**

A. LALLA & H. MÜLLER-BUSCHBAUM . . . . . 605

**Stabilisation du ruthénium (V) au sein des phases Ln<sub>2</sub>LiRuO<sub>6</sub> (Ln = TERRE RARE).**

E. O. OH-KIM, G. DEMAZEAU & P. HAGENMULLER . . . . . 613

**Substitutions cationiques et interactions magnétiques dans les perovskites hexagonales fluorées. IV. Les systèmes CsNi<sub>1-x</sub>Ca<sub>x</sub>F<sub>3</sub> et Cs<sub>1-x</sub>Rb<sub>x</sub>Ni<sub>1-x</sub>Ca<sub>x</sub>F<sub>3</sub>, avec 0 ≤ x ≤ 1.**

A. TRESSAUD, G. DEMORTAIN, F. BOURÉE-VIGNERON & J. DARRIET . . . . . 621

**Structure de Bi<sub>2</sub>(CrO<sub>4</sub>)<sub>2</sub>Cr<sub>2</sub>O<sub>7</sub>.**

Y. GERAULT, A. RIOU, Y. CUDENNEC & A. BONNIN . . . . . 631

**Elaboration de sols stanniques à partir de complexes stannitartriques.**

J. MAZIÈRES, M. BEAOUI, J. LEMERLE & J. LEFEBVRE . . . . . 641

**The oxidation of some transition metal nitrides and carbides.**

J. N. CLARK, D. R. GLASSON & S. A. A. JAYAWEERA . . . . . 654

**Activation du frittage sous charge du nitre de silicium par un prétraitement thermique.**

Y. ZHANG, D. BERNACHE-ASSOLLANT & S. PIEKARSKI . . . . . 667

**Phase diagrams relevant for sintering aluminum nitride based ceramics.**

J. C. SCHUSTER . . . . . 676

**Frittage et propriétés du nitre d'aluminium préparé par réaction NH<sub>3</sub>/Al<sub>2</sub>O<sub>3</sub>.**

J. JARRIGE, J. MEXMAIN, J. P. MICHELET, J. GUYADER, Y. LAURENT & H. L. BODO . . . . . 687

**Hot pressing of silicon nitride with mixed rare-earth oxide additives.**

E. RAPOORT, C. BRODHAG & F. THEVENOT . . . . . 697

**Some aspects of the formation of ε-Ti<sub>2</sub>N.**

W. LENGAUER & P. ETTMAYER . . . . . 707

**Nouveaux résultats sur les apatites azotées. II. Teneur en azote et stabilité des composés purement lanthanidiques.**

J. GAUDÉ . . . . . 714

**Propriétés thermodynamiques molaires et transformations dans la magnétite non stœchiométrique en équilibre avec les wüstites.**

P. VALLET & C. CAREL . . . . . 719

# Preparation, crystal structure, and thermal behaviour of potassium ozonide

by

**Wolfgang SCHNICK and Martin JANSEN**

Institut für Anorganische Chemie und SFB 173,  
Callinstr. 9, D-3000 Hannover 1, Federal Republic of Germany,

*Dedicated to Professor Albrecht Rabenau on the occasion of his 65th birthday.*

**ABSTRACT.** — The preparation of pure samples of potassium ozonide ( $KO_3$ ) in gramm-amounts was achieved by reaction of gaseous ozone/oxygen mixtures (2 Vol.-%  $O_3$ ) with potassium hyperoxide in a temperature-controlled ( $T = +10$  to  $-50^\circ C$ ) fluidized bed reactor followed by extraction with liquid ammonia. According to thermal (DT, TG) investigations  $KO_3$  is metastable at ambient conditions. Longtime storage is possible in a dry inert atmosphere below  $-20^\circ C$ . The crystal structure of  $KO_3$  was solved by single-crystal X-ray techniques. Lattice constants were determined from the X-ray powder pattern of  $KO_3$  which was indexed in agreement with the single-crystal results.

Bond angle and distance in the ozonide anion ( $O_3^-$ ) are  $113.5(1)^\circ$  and  $134.6(2)$  pm, respectively. The crystal structures of  $KO_3$ ,  $RbO_3$ ,  $H-CsO_3$ ,  $T-CsO_3$ ,  $CsNO_2$  and  $BaS_3$  are related to each other and derive from the CsCl-type of structure.

**RÉSUMÉ.** — Des échantillons purs d'ozonure de potassium ( $KO_3$ ), dans des gammes de masse de l'ordre du gramme, ont été préparés par réaction d'un mélange gazeux ozone/oxygène (2%  $O_3$  en volume) avec l'hyperoxyde de potassium dans un réacteur en couche fluide à température variable ( $T = +10$  à  $-50^\circ C$ ), suivie d'une extraction avec de l'ammoniac liquide. D'après les études thermiques (ATD, TG)  $KO_3$  est métastable dans les conditions normales de température et de pression. La conservation est possible dans une atmosphère sèche et inerte en dessous de  $-20^\circ C$ . La structure cristalline de  $KO_3$  a été déterminée par diffraction des rayons X sur un monocristal. Les paramètres du réseau ont été déterminé d'après le diagramme de poudre de  $KO_3$ , indexé en accord avec les résultats de la technique du monocristal.

La distance entre les atomes d'oxygène et l'angle des liaisons dans les anions ozonide ( $O_3^-$ ) sont respectivement  $134.6(2)$  pm et  $113.5(1)^\circ$ . Les structures cristallines de  $KO_3$ ,  $RbO_3$ ,  $H-CsO_3$ ,  $T-CsO_3$ ,  $CsNO_2$  et  $BaS_3$  sont corrélées et dérivent de la structure CsCl.

## INTRODUCTION

Since the first reports by Wurtz [1] and Baeyer and Villiger [2] on the formation of new compounds during the reaction of ozone with alkalihydroxides, several attempts have been undertaken to clarify their

nature [3, 4]. These efforts however, have been only partly successful. So far, no reliable structural data has become available and no synthetic route has been developed, which allows syntheses of pure samples on a preparative scale.

Concerning the crystal structure of  $\text{KO}_3$ , two proposals have been made, based on X-ray powder data on samples containing  $\text{KOH}$  and  $\text{KO}_2$  as impurities. Zhdanova and Zvonkova suggested that  $\text{KO}_3$  is isostructural to  $\text{KN}_3$  and is likely to contain a linear  $\text{O}_3$ -group [4]. Azároff and Corvin report a similar unit cell, a bent anion with an angle of  $100^\circ$  and a separation between adjacent oxygen atoms of 119 pm which is smaller than in ozone itself and is thus rather unreasonable [3 a].

In advance of testing a more general application of the ozonides in preparative inorganic or organic chemistry and for further discussion of the bonding properties, it seemed necessary to us to develop and optimize a procedure for the preparation of pure ozonides in gramm-amounts and to determine the crystal structures with single crystal methods. In this paper we report our results on preparation, crystal structure, and properties of potassium ozonide.

## EXPERIMENTAL

### *Synthesis*

From the methods proposed earlier for synthesizing  $\text{KO}_3$  using  $\text{KOH}$  [5] or  $\text{KO}_2$  [3 g] as starting material, ozonisation of powdered hyperoxide with gaseous  $\text{O}_3/\text{O}_2$ -mixtures ( $\sim 2 \text{ Vol. } - \% \text{ O}_3$ ) was deemed most suitable. Potassium hyperoxide was prepared by direct oxidation of pure potassium metal with molecular oxygen according to the method given by Helms and Klemm [6]. Peroxide-free samples were only obtained after treating the crude product at  $450^\circ\text{C}$  under elevated  $\text{O}_2$ -pressure ( $6 \cdot 10^7 \text{ Pa}$ , reaction-time: 3 d) in an autoclave.

The reaction of ozone with  $\text{KO}_2$  according to the equation (i)



may be subdivided into the dissociation of ozone



producing monooxygen diradicals, which immediately react with hyperoxide forming ozonide



Because dissociation of ozone (ii), as a metastable compound, is kinetically controlled raising the temperature increases the production rate of O-radicals which themselves recombine to dioxygen in an exothermic reaction competitive to the ozonide formation.

With respect to decomposition into  $\text{KO}_2$  and  $\text{O}_2$ , potassium ozonide is metastable. At about  $45^\circ\text{C}$  the rate of  $\text{O}_2$  evolution reaches a maximum (see below). So, during ozonisation, heating of the sample due to the exothermic reactions mentioned above must be suppressed by external cooling. On the other hand heterogeneous reaction and diffusion in the solid state are necessary steps during the formation of  $\text{KO}_3$  according to equation (i), and need a

minimum temperature of about 10°C for acceptable reaction rates. These two conflicting aspects demand a proper temperature control. This was achieved by using a small cylindrical fluidized bed reactor ( $\varnothing = 30$  mm) equipped with a cooling jacket, which allowed a temperature control in the range -75 to +30°C. When starting the reaction at room temperature the red colour of  $KO_3$  appeared almost immediately; because of the self-heating reaction, however, the initially formed  $KO_3$  decomposed soon. Upon cooling formation of  $KO_3$  started again in the outer parts of the samples (next to the cooled wall); within 1 hour the reaction zone moved through the sample while the temperature was reduced stepwise to -50°C. As in no case complete reaction of the hyperoxide was observed, enrichment and purification by extraction with and recrystallization from liquid ammonia was carried out. The remaining hyperoxide may be ozonized so that, by repeated ozonization and subsequent extraction, quantitative yields on the basis of the initial amount of  $KO_2$  are possible. All substances were handled during the whole procedure under carefully inert conditions. A detailed description of the equipment used is given elsewhere [7 a, b].

Viable crystals for single-crystal X-ray investigations were obtained by very slow evaporation (2 hrs.) of liquid ammonia from the potassium ozonide solution. The product crystallized in transparent dark red crystals, which are extremely reactive upon contact with water and carbon dioxide.

#### *Analyses*

The active oxygen of the ozonide samples was determined by measuring the loss of weight during thermal decomposition to hyperoxide. The content of active oxygen was found to be 98,7 (13) % of the theoretical value (esd in brackets). The samples were then dissolved in water and potassium was determined by precipitation as potassium-tetraphenylborate according to the method given by Geilmann and Gebauhr [8]. The potassium content was found to be 45.0% (theoretically: 44.9%).

#### *Thermal decomposition*

The thermal behavior of potassium ozonide was studied applying DTA-TG-methods and various heating rates. It was thus found that  $KO_3$  decomposes exothermally at ambient conditions. Extrapolated to a heating rate of 0 K/min the decomposition rate reaches its maximum at 45°C under 1 atmosphere Argon (cf. Fig. 1). Thermal decomposition of  $KO_3$  leads quantitatively to the corresponding hyperoxide.

#### *Structure determination*

A single crystal of  $KO_3$  was wedged in a capillary tube under dry argon. After sealing, the tube was mounted on an AED2 Siemens-Stoe four-circle-diffractometer. Because of its thermal instability (see before) all X-ray measurements on the  $KO_3$ -crystal were undertaken at -20°C using the Stoe low temperature attachment.

Preliminary examinations indicated the crystal to be tetragonal, space group  $I4/m\ cm$ . The unit cell dimensions (-20°C) were obtained by least-squares-fit to the setting angles of 56 reflections measured in positive and negative  $2\theta$ . The data are summarized in Table I along with the details of the treatment of the intensity data.

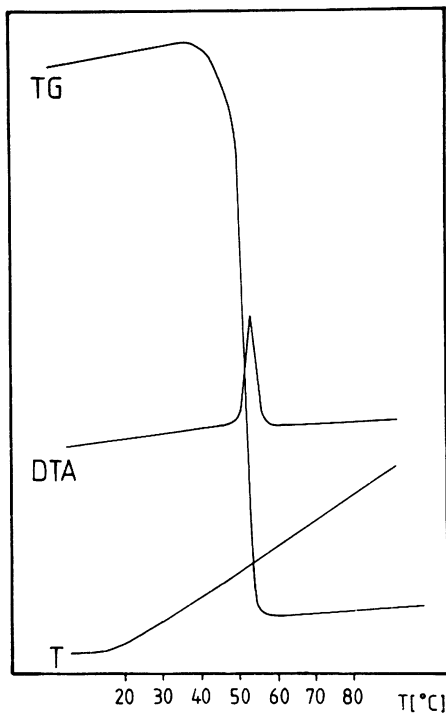


Fig. 1. — DTA-TG-Curve for  $\text{KO}_3$ ;  
heating rate : 1K/min.

Four standard reflections were measured every 60 minutes and showed no significant change in intensity. A total of 2,509 reflections were measured. The reflections were considered unobserved for  $|F_0|$  less than  $\sigma(F_0)$ . The intensities were corrected for Lorentz and polarization effects. Numerical absorption correction was applied.

The initial positions of potassium- and oxygen-atoms were determined by direct methods [9] and refined by a least-squares procedure minimizing the functions  $\sum w |F_0| - |F_c|^2$  with final convergence to

$$R = \sum |F_0| - |F_c| / \sum |F_0| = 0.035$$

and

$$R_w = \sum \sqrt{w} |F_0| - |F_c| / \sum \sqrt{w} |F_0| = 0.02 (w = 1/\sigma^2(F_0)).$$

Scattering factors for all atoms were taken from ref. [10]. The final parameters are given in Table II and selected bond distances and angles in Table III.

TABLE I  
*Data for crystal structure analysis.*

Formula	KO <sub>3</sub>
M	87.1
Crystal system	Tetragonal
Space group	14/m c m
a/pm	863.58(10)
c/pm	714.06(8)
V/pm <sup>3</sup> · 10 <sup>+6</sup>	532.52
Z	8
D <sub>c</sub> /g · cm <sup>-3</sup>	2.173
μ(Mo-K <sub>α</sub> )/cm <sup>-1</sup>	16.10
2θ range/°	2 ≥ 2θ ≥ 70
Transmission coefficient	0.78-0.87
Approx. crystal size/mm	0.06 × 0.07 × 0.06
Data collection instrument	Siemens-Stoe AED2
Measuring mode	ω-Scan
Temperature/°C	-20
No. of data measured	2509
No. of unique reflections	341
No. of observed data	309
Criterion for observed	n = 1.0
I ≥ n σ(I)	
Merging r-value	0.062
No. of parameters refined	15
R	0.035
R <sub>w</sub> ; w = 1/σ <sup>2</sup> (F)	0.020

### Powder diffraction

In order to determine accurate lattice constants of KO<sub>3</sub> the X-ray powder diffraction pattern of this compound was recorded by using a Guinier-Simon [11] camera (T = -25°C) and monochromated Cu K<sub>α1</sub> radiation ( $\lambda = 154.056$  pm). If a tetragonal cell with  $a = b = 864.5$  (6) pm and  $c = 714.43$  (8) pm, is chosen, the pattern can be indexed as shown in Table IV. All observed *d*-spacings and intensities are in good agreement with the values calculated from the results of the single-crystal-investigations. The uncertainties concerning the powder diffraction pattern of KO<sub>3</sub> due to the contradictory results of prior investigations [3 a, 4], can now be eliminated.

### RESULTS, DISCUSSION

Applying the improved procedure reported in this paper pure samples (as characterized by chemical analysis and X-ray powder diffraction) of potassium ozonide in large amounts are now accessible. KO<sub>3</sub> is metastable with respect to decomposition into KO<sub>2</sub> and O<sub>2</sub> under ambient conditions.

TABLE II

*Refined Positional and Thermal Parameters for KO<sub>3</sub> (with esd's in parentheses) (a).*

Atom	x	y	z	U <sub>11</sub>	U <sub>22</sub>
K(1)	0	0	0.25	0.0260(2)	0.0260(2)
K(2)	0	0.5	0.25	0.0326(3)	0.0326(3)
O(1)	0.2807(1)	0.2193(1)	0	0.0263(5)	0.0263(5)
O(2)	0.2489(1)	0.0667(1)	0	0.0291(5)	0.0263(6)
Atom	U <sub>33</sub>	U <sub>12</sub>	U <sub>13</sub>	U <sub>23</sub>	
K(1)	0.0206 (8)	0	0	0	
K(2)	0.0256(10)	0	0	0	
O(1)	0.0758(13)	0.0004(6)	0	0	
O(2)	0.0398 (6)	-0.0076(5)	0	0	

(a) Anisotropically refined thermal parameters defined as

$$\exp[-2\pi^2[U_{11}h^2a^{*2}+U_{22}k^2b^{*2}+U_{33}l^2c^{*2}+2U_{12}hk a^*b^*+2.U_{13}hl a^*c^*+2.U_{23}.K.l.b^*c^*]\text{\AA}^2].$$

TABLE III

*Selected Interatomic Distances (pm) and Angles (deg) for KO<sub>3</sub>.*

O1—O2	134.6 (2)	O2—O1—O2'	113.5 (1)
Shortest intermolecular O—O-distance :			
O1—O2	301.1 (4)		
Potassium-oxygen distances :			
K1—O2	285.3 (3)	(eight times)	
K2—O2	286.7 (3)	(eight times)	
K2—O1	321.9 (4)	(four times)	
K1—O1	355.7 (5)	(eight times)	

The decomposition rate decreases with decreasing temperature, so a long-time storage of potassium ozonide is possible at -20°C under dry argon.

The crystal structure of potassium ozonide (cf. Fig. 2) consists of K<sup>+</sup> and O<sub>3</sub><sup>-</sup> ions. Based on this investigation and our recent results on RbO<sub>3</sub> [7] definite bond lengths and angles within the O<sub>3</sub><sup>-</sup>-anion can be given : the mean values from these two independent determinations are 134.4(7) pm and 113.6(5)<sup>o</sup>, respectively. The small difference between the individual data (KO<sub>3</sub> c.f. Table III, RbO<sub>3</sub>: d<sub>O-O</sub>=134.3(7) pm, <O—O—O=113.7(5)<sup>o</sup>) indicate that influence of the crystal fields on the geometry of O<sub>3</sub><sup>-</sup> are clearly negligible in both cases. As compared to

TABLE IV

*Observed and Calculated X-ray Powder Pattern  
for KO<sub>3</sub> (T = -25°C)*

<i>h k l</i>	<i>d<sub>c</sub></i>	<i>d<sub>0</sub></i>	<i>I<sub>c</sub></i>	<i>I<sub>0</sub></i>
1 1 0	6,113		0,1	
2 0 0	4,323	4,325	162,7	15
0 0 2	3,572		18,5	
2 1 1	3,400	3,404	348,4	30
1 1 2	3,084		0	
2 2 0	3,058	3,057	188,5	15
2 0 2	2,754	2,754	1 000,0	100
3 1 0	2,734		0,4	
2 2 2	2,3225	2,3220	352,3	30
3 2 1	2,2733	2,2737	85,8	10
3 1 2	2,1712		0,3	
4 0 0	2,1614	2,1621	262,5	25
3 3 0	2,0378		1,2	
2 1 3	2,0277	2,0283	57,3	5
4 1 1	2,0120		5,5	
4 2 0	1,9332	1,9330	138,8	12
4 0 2	1,8493		15,4	
0 0 4	1,7862	1,7863	112,4	10
3 3 2	1,7700		1,3	
1 1 4	1,7147		0	
4 2 2	1,7002	1,7004	151,6	15
5 1 0	1,6956		0,1	
3 2 3	1,6897		25,7	
4 3 1	1,6806		3,0	
2 0 4	1,6507		20,7	
4 1 3	1,5738		1,9	
5 2 1	1,5664		13,9	
2 2 4	1,5421		38,9	
5 1 2	1,5318		0,2	
4 4 0	1,5284		34,5	
3 1 4	1,4953		0,1	
5 3 0	1,4827		1,4	
6 0 0	1,4409		1,0	
4 4 2	1,4051		31,7	
4 3 3	1,3992		1,4	
6 1 1	1,3940		20,4	
4 0 4	1,3768	1,3767	93,7	10
5 3 2	1,3694		2,0	
6 2 0	1,3670	1,3670	52,0	5
3 3 4	1,3432		0,4	
2 1 5	1,3403		9,8	
6 0' 2	1,3363	1,3362	107,4	10
5 2 3	1,3312		7,0	
5 4 1	1,3267		3,1	
4 2 4	1,3119	1,3119	69,5	5

ozone ( $d_{O-O} = 128$  pm) the bond distance is enlarged. This is expected, as the additional electron in O<sub>3</sub><sup>-</sup> occupies the antibonding 2  $b_1$  molecular orbital and thus the bond-order *n* is decreased from 1.5(O<sub>3</sub>) to 1.25(O<sub>3</sub><sup>-</sup>).

The relation found between bond order and bond lengths fits well into the scheme of the corresponding relations for other homoatomic bonds of oxygen (Fig. 3). In spite of the decrease of the O—O—O angle to  $113.6^\circ$  (ozone:  $116.5^\circ$ ) repulsion between the nonbonded terminal oxygen atoms is relaxed, as can be seen from an increase of their separation by 6 pm. So the variation in the bonding angle is caused mainly by the different electronic structures, an observation which is in accordance with the opinion expressed by Peyerimhoff and Buenker [17] that in triatomic bent molecules with constituent atoms of nearly equal electronegativities such geometrical variations are at most only to a negligible extent due to the repulsive forces mentioned.

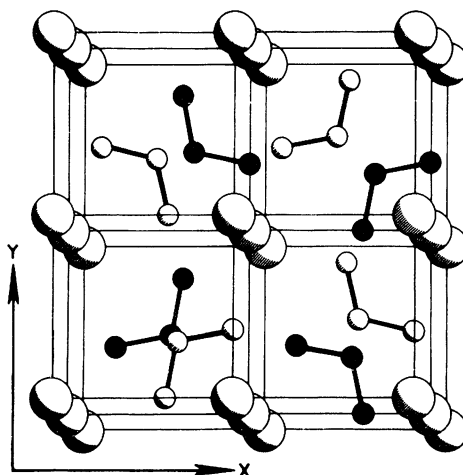


Fig. 2. — Crystal structure of  $\text{KO}_3$ . View along [001].  
Large spheres: K; small spheres: O (shaded at  $z = 0$ , otherwise  $z = 1/2$ ).

As can be deduced from Figure 2 the packing of the anions and cations in the crystal structure of potassium ozonide is in principle the same as in cesium chloride. This general arrangement is adopted by several other salts of similar composition, e. g.  $\text{BaS}_3$  [18],  $\text{RbO}_3$  [7],  $\text{H}-\text{CsO}_3$  [19] and  $\text{H}-\text{CsNO}_2$  [20]. Approximating the triatomic bent anions as spheres the structural relations may be expressed by group-subgroup relationships [21] (cf. Fig. 4). In  $\text{H}-\text{CsO}_3$  and  $\text{H}-\text{CsNO}_2$  which are isostructural the anions are orientationally disordered. So in the average of time and space the crystals exhibit cubic symmetry and the structure of these two representatives may be seen as the « aristotype » of this structural family.

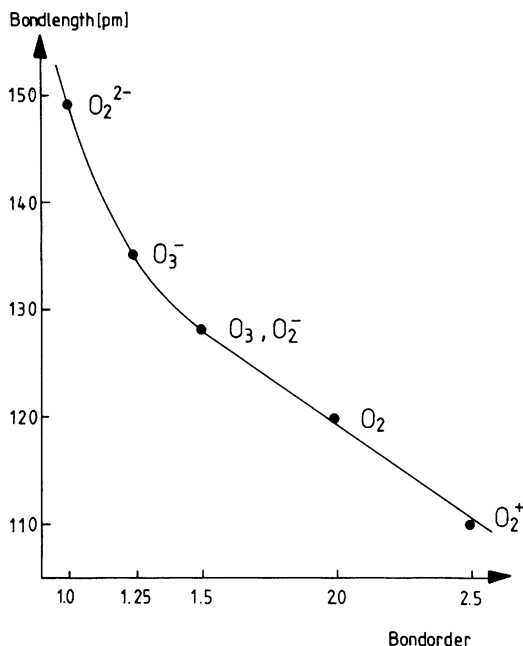


Fig. 3. — Relation between bond length  $d$  and bond order  $n$  in homoatomic oxygen molecules:  $O_2^+$  [12],  $O_2$  [13],  $O_2^-$  [14],  $O_3$  [15],  $O_2^{2-}$  [16], and  $O_3^-$ .

In  $KO_3$  the shortest contacts between oxygen and potassium are those at the terminal O-atoms of the ozonide group, with the resulting distances (285 and 287 pm) corresponding to the sum of the ionic radii of potassium and oxygen (289 pm) [22]. This structural feature allows qualitative conclusions on the polarity of the ozonide anion to be drawn: in agreement with SCF-MO-calculations by Cosgrove and Collins [23], the terminal oxygen atoms seem to be polarized negatively. The calculated electron density coefficients of the  $2 b_1$ -molecular orbital, which accommodates the nineteenth valence electron were found to be 0.372 for the terminal and 0.255 for the central oxygen atoms. Striving towards K—O bonding contacts mentioned above, the ozonide ions are shifted from the centre of the polyhedron formed by the eight nearest potassium ions by the considerable amount of 86.7 pm.

According to the group-subgroup-relations between the crystal structures of  $KO_3$  and  $RbO_3$  the rubidium compound is a more distorted variant of the  $CsCl$ -type structure. This distortion may be caused by the fact that

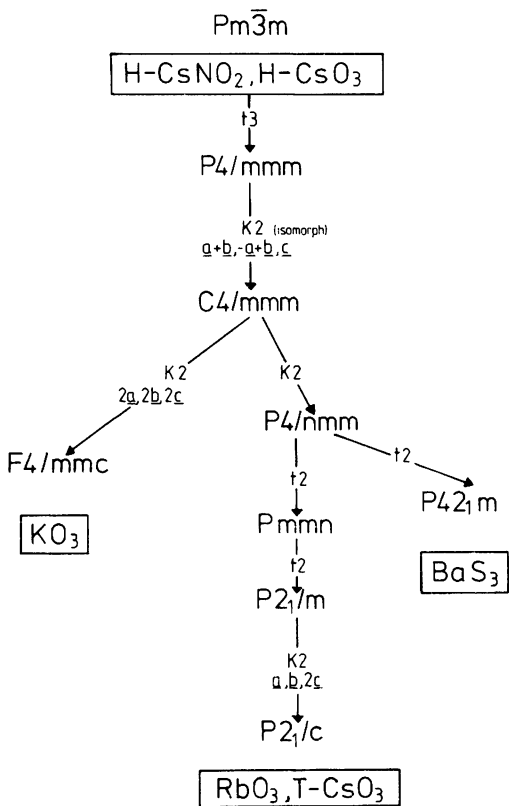


Fig. 4. — Group-subgroup relations between the crystal structures of  $\text{KO}_3$ ,  $\text{RbO}_3$ ,  $\text{H}-\text{CsO}_3$ ,  $\text{T}-\text{CsO}_3$ ,  $\text{CsNO}_2$ , and  $\text{BaS}_3$ .

the larger Rb-cations require and obtain a higher coordination number by adjacent oxygen atoms ( $\text{KO}_3$ : 8;  $\text{RbO}_3$ : 9).

The ozonide groups are arranged in a strictly ordered manner forming layers parallel to (001) (cf. Fig. 2). This type of ordering causes a tetragonal distortion of the CsCl analogous units from " $c/a$ " = 1.0 to 0.83 and is understandable in terms of polar interactions between positively and negatively polarized oxygen atoms of adjacent  $\text{O}_3^-$ -ions. Covalent inter-actions along with spin pairing can be ruled out as the shortest intermolecular O—O-separations between neighbouring  $\text{O}_3^-$ -ions are 301 pm, and thus in the range of van der Waals contacts [24]. Moreover, preliminary measurements of the magnetic susceptibility show paramagnetic behavior down to 21 K [25].

*Acknowledgement.* — Financial support by the Deutsche Forschungsgemeinschaft and Fonds der Chemischen Industrie is gratefully acknowledged.

## REFERENCES

- [1] C. A. WURTZ, *Dictionnaire de Chimie pure et appliquée*, 1868, **II**, p. 721.
- [2] A. BAAYER and V. VILLIGER, *Chem. Ber.*, **35**, 1902, p. 3038.
- [3] (a) L. V. AZÁROFF and I. CORVIN, *Proc. Natl. Acad. Sci. U.S.A.*, **49**, 1963, p. 1;  
 (b) V. A. SARIN, V. Y. DUDAREV, and M. S. DOBROLYUBOVA, *Kristallografiya*, **19**, 1974, p. 74; (c) P. SMITH, *J. Phys. Chem.*, **60**, 1956, p. 1471; (d) L. PAULING, *The Nature of the Chemical Bond*, Cornell Univ. Press, New York, 1980, p. 354; (e) S. SCHLICK, *J. Chem. Phys.*, **56**, 1972, p. 654; (f) A. D. McLACHLAN, M. C. R. SYMONS and M. G. TOWNSEND, *J. Chem. Soc.*, 1959, p. 952; (g) I. I. VOL'NOV, E. I. SOKEVNIN and V. V. MATVEEV, *Izv. Akad. Nauk. S.S.R.*, **6**, 1962, p. 1127; (h) I. I. VOL'NOV, M. S. DOBROLYUBOVA and A. B. TSENTSIPER, *Izv. Akad. Nauk S.S.R. Ser. Khim.*, **9**, 1966, p. 1611.
- [4] G. S. ZHADANOVA and Z. V. ZVONKOVA, *Zh. Fiz. Khim.*, **25**, 1951, p. 100.
- [5] T. P. WHALEY and J. KLEINBERG, *J. Amer. Chem. Soc.*, **73**, 1951, p. 79.
- [6] (a) A. HELMS and W. KLEMM, *Z. Anorg. Allg. Chem.*, **242**, 1939, p. 33; (b) K. WAHL, *Dissertation*, Universität Münster, 1954.
- [7] (a) W. SCHNICK and M. JANSEN, *Z. Anorg. Allg. Chem.*, **532**, 1986, p. 37. (b) W. SCHNICK and M. JANSEN, *Angew. Chem. (Int. Ed.)*, **24**, 1985, p. 54.
- [8] W. GEILMANN and W. GEBAUHR, *Z. Anal. Chem.*, **139**, 1953, p. 161.
- [9] Computations were carried out on a Data General ECLIPSE S/140 by using the Stoe STRUCSY program package (rev. 1), Darmstadt, 1984.
- [10] "International Tables for X-Ray Crystallography", Kynoch Press, Birmingham, **4**, 1974.
- [11] A. SIMON, *J. Appl. Cryst.*, **3**, 1970, p. 11.
- [12] B. G. MÜLLER, *J. Fluorine Chem.*, **17**, 1981, p. 489.
- [13] S. I. MILLER and C. H. TOWNES, *Phys. Rev.*, **90**, 1953, p. 537.
- [14] S. C. ABRAHAMS and J. KALNAJS, *Acta Cryst.*, **8**, 1955, p. 503.
- [15] R. H. HUGHES, *J. Chem. Phys.*, **24**, 1956, p. 131.
- [16] S. C. ABRAHAMS and J. KALNAJS, *Acta Cryst.*, **7**, 1954, p. 838.
- [17] S. D. PEYERIMHOFF and R. J. BUENKER, *J. Chem. Phys.*, **47**, 1967, p. 1953.
- [18] H. G. V. SCHNERING and NGOH-KHANG GOH, *Naturwissenschaften*, **61**, 1974, p. 272.
- [19] W. HESSE and M. JANSEN, *unpublished work*.
- [20] P. W. RICHTER and C. W. F. T. PISTORIUS, *J. Solid State Chem.*, **5**, 1972, p. 276.
- [21] (a) J. NEUBÜSER and H. WONDRATSCHEK, *Kristall und Technik*, **1**, 1966, p. 529;  
 (b) H. BÄRNIGHAUSEN, *Com. Math. Chem.*, **9**, 1980, p. 139.
- [22] R. D. SHANNON and C. T. PREWITT, *Acta Cryst.*, **B25**, 1969, p. 925.
- [23] M. M. COSGROVE and M. A. COLLINS, *J. Chem. Phys.*, **52**, 1970, p. 989.
- [24] N. W. ALCOCK, *Adv. Inorg. Chem. Radiochem.*, **15**, 1972, p. 1.
- [25] H. LUEKEN, M. DEUSSEN, M. JANSEN, W. HESSE and W. SCHNICK., Submitted for publication in *Z. Anorg. Allg. Chem.*

(Received June 24 1987.)